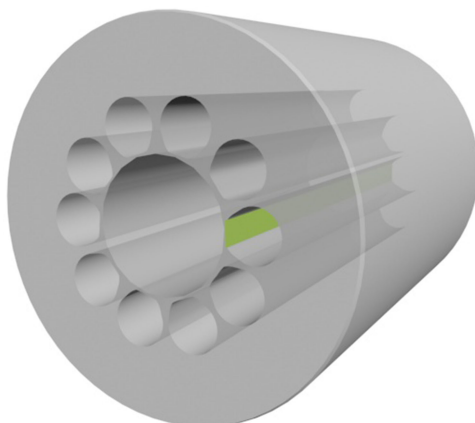


# Research on Fabrication and Performance of Hollow-Core Anti-Resonant Fiber Coated With Copper Film

Volume 12, Number 3, June 2020

Meng Wu  
Boyao Li  
Jialong Li  
Guizhao Zhou  
Changming Xia  
Zhiyun Hou



---

DOI: 10.1109/JPHOT.2019.2954534

# Research on Fabrication and Performance of Hollow-Core Anti-Resonant Fiber Coated With Copper Film

Meng Wu<sup>1,2</sup> Boyao Li<sup>1,2</sup> Jialong Li<sup>1,2</sup> Guiyao Zhou<sup>1,2</sup>  
Changming Xia,<sup>1,2</sup> and Zhiyun Hou<sup>1,2</sup>

<sup>1</sup>Guangzhou Key Laboratory for Special Fiber Photonic Devices, South China Normal University, Guangzhou 510006, China

<sup>2</sup>Guangdong Province Key Laboratory of Nano-Photonic Functional Materials and Devices, South China Normal University, Guangzhou 510006, China

DOI:10.1109/JPHOT.2019.2954534

This work is licensed under a Creative Commons Attribution 4.0 License. For more information, see <http://creativecommons.org/licenses/by/4.0/>

Manuscript received September 7, 2019; revised October 30, 2019; accepted November 15, 2019. Date of publication November 27, 2019; date of current version June 26, 2020. This work was supported in part by the National Natural Science Foundation of China under Grants 61575066, 61527822, and 61735005, in part by Guangdong Natural Science Foundation under Grant 2017A030313333, in part by the Science and Technology Program of Guangzhou, China, under Grant 201707010133, in part by the Science and Technology Planning Project of Guangdong Province under Grant 2017KZ010201, in part by GDUPS (2017), in part by the National Key Research and Development Program of China under Grant 2018YFB0407400, in part by The Innovation Project of Graduate School of South China Normal University under Grant 2018LKXM040, and in part by the SCNU Study Abroad Program for Elite Postgraduate Students, China. Corresponding author: Meng Wu (e-mail: houzhiyun@163.com).

**Abstract:** A Hollow-core Anti-resonant Fiber (ARF) has many advantages in device applications, such as low cladding density, low nonlinearity, high damage threshold, and excellent polarization characteristics by adjusting the structure and filling a metal. A method of on-line copper coating on the inner hole of hollow-core anti-resonant fiber cladding during drawing is proposed in this paper, and the related polarization characteristic of the ARF is studied. The theoretical and experimental results show that the ARF has good polarization characteristics after coating due to the coupling of copper film and core mode. Polarized light at 860 nm shows the best polarization characteristics. When the ARF is 1 mm, 1.5 mm, and 2 mm in length, its crosstalk is more than 20 dB which works well in communications applications. These characteristics indicate that the ARF coated copper film has a good application prospect in the field of polarization communication.

**Index Terms:** Polarization characteristics, anti-resonant fiber, surface plasmon resonance, copper film.

## 1. Introduction

In recent years, the fabrication of miniaturized and integrated functional microstructured optical fiber (MOF) devices has attracted great attention and exponentially risen for its flexible and controllable structure, adjustable dispersion and birefringence [1], [2]. Typically, various theoretical studies based on MOF functional devices have been successfully developed [3], [4]. The ingenious combination of surface plasmon and microstructured optical fibers provides a broad stage for the development of special optical fiber functional devices, such as an optical switch, sensors and polarizing filter [5]–[7]. However, due to the incomplete development, it cannot be well applied in some specific bands and scenarios.

In order to achieve good polarization characteristics of optical fiber devices, some researchers begin to combine metal with optical fiber finding it can improve the polarization of optical fiber devices effectively [8]–[12]. It is because surface plasmon resonance (SPR) between metal and dielectric can be produced when free electrons interact with the light on the metal surface. In 2012, Lee embedded two parallel gold nanowires in a MOF to achieve polarization effect [8]. In 2013, Xue used the finite element method to study the polarization filtering characteristics of gold-plated and liquid-filled photonic crystal fibers [9]. The polarization filtering properties of square lattice photonic crystal fibers with large diameter gold-plated holes were studied by Zi in 2015 [10]. In 2016, Li proposed an improved design of the MOF filter based on SPR [11]. Basak studied the polarization properties of suspended core microstructured optical fibers (SC-MOFs) with hexagonal lattice structure, having a single gold-filled hole along the horizontal axis most recently [12]. Although these reported devices have good polarization characteristics, they are only capable of working in common communication band instead of high-power transmission and other communication bands.

With the development of optical fiber technology, hollow-core optical fibers exhibit many superior properties, such as high damage threshold, low nonlinearity, transmission bandwidth, etc. Therefore, some people begin to use hollow fibers to achieve polarization characteristics [13]. Mousavi systematically studied different approaches to introduce high birefringence and high polarization extinction ratio in hollow-core anti-resonant fibers in 2016 [14]. In 2018, Wei proposed a polarization filter and a polarization-preserving negative curvature fiber, in which two nested resonators were added to a standard negative curvature fiber with a ring [15]. In the same year, Yan proposed a novel dual-ring hollow ARF, which can achieve single-polarization guidance [16]. In order to obtain wider bandwidth of optical fiber polarizers, Wolinski studied the polarization effect in fiber waveguides with a liquid core in 2000 [17]. In 2011, Qian designed a new type of polarizer by filling part of the hollow photonic bandgap fiber (PBGF) with liquid [18]. In 2015, Mohamed Farhat O designed electrically adjustable and rotating polarizers by infiltrating liquid crystals into MOFs [19]. Thus, the polarization devices based on the Hollow-core Anti-resonant Fiber (ARF) have great potential application value, but they are still in the theoretical stage [13]–[19].

Herein, a method of on-line copper coating on the inner surface of fiber cladding holes is proposed by combining ARF and SPR. This method can achieve real-time, convenient, simple and efficient coating process. Besides, the final sample was detailed analyzed. The theoretical and experimental results show that the device has good polarization and crosstalk characteristics. Polarized light at 860 nm shows the best polarization characteristics. When the ARF is 1 mm, 1.5 mm, and 2 mm in length, its crosstalk is more than 20 dB which works well in communications applications. These characteristics indicate that the ARF coated copper film has a good application prospect in the field of polarization communication. The resonance band is 800 nm to 900 nm and the crosstalk is more than 20 dB. The experimental results are basically consistent with the theory. These results are of great significance for the development of high damage threshold and multi-functional optical fiber devices in the fields of optical communications, optical sensors, and optical functional devices.

## 2. Design and Fabrication

To destroy the symmetry of the optical fiber and increase the loss in one direction, a copper film is coated on one of the holes of the optical fiber cladding according to the theoretical design (Fig. 1a). Due to the high technical difficulty of metal coating on micron inner holes, an on-line coating technology for optical fiber drawing process is proposed. Firstly, we fill 10 capillaries into the outer tube as shown in Fig. 1b. In order to realize the coupling between the core mode and surface plasmon polariton (SPP) mode, a copper film with a thickness of 10  $\mu\text{m}$  is attached to one of the holes in the cladding of optical fiber preform. Because the melting point of copper is 1083.4 °C and the boiling point is 2567 °C, when the prefabricated rod is pulled at 1800 °C of the fiber drawing tower and the copper foil will melt and evaporate partially (Fig. 1c). And then the copper film will be coated on the inner wall of the air hole as shown in Fig. 1d. Due to the limitation of the measuring instrument, we cannot see the Cu film clearly in the end-face diagram under the

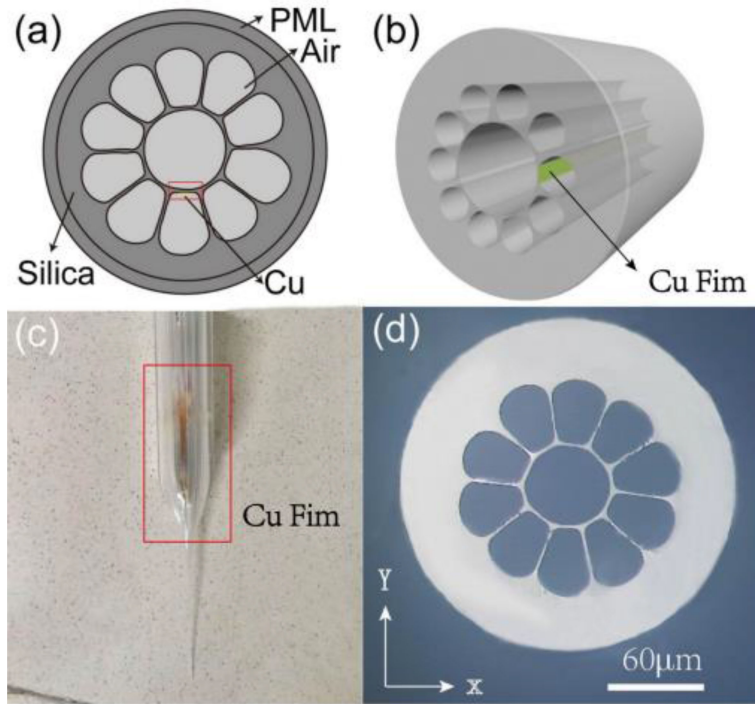


Fig. 1. Fabrication process of hollow core fiber coated with copper film. (a) Design of optical fiber end diagram. (b) 3-D model of fiber preform. (c) Residual prefabricated rods. (d) The real copper coated with Cu after drawing and SPR effect proves the existence of copper film.

microscope. However, the corresponding experimental results show that Cu does exist and SPR occurs. According to the scale ratio, The radius of the inner core and the outer cladding of the ultimate optical fiber is are 24.5 um and 103 um, respectively.

The confinement loss of guided mode is an important parameter for evaluating polarizer characteristics. And it can be expressed by the following formulas:

$$L = 8.686 \times \frac{2\pi}{\lambda} \text{Im}(n_{\text{eff}}) \times 10^4 \quad (1)$$

Where,  $\text{Im}(n_{\text{eff}})$  represents the imaginary part of the effective refractive index, and the unit of limiting loss is dB/cm [20], [21].

The fiber we presented above is calculated by the modal calculator based on the full vector finite element method. Considering the accuracy and efficiency of calculation, the calculation model is a two-dimensional model. Fig. 2 shows the polarization losses of x-polarized mode and y-polarized mode. Because the copper film is in the Y direction of the polarizer, it is obvious that the polarizer has strong polarization phenomenon in the Y direction.

In Fig. 2, there is a strong coupling between the SPP mode and the core mode in the Y direction. The plasma mode on the metal surface is coupled with the core mode in the optical fiber. Because we deposit metal in one direction, the coupling loss of the core-mode in that direction will increase, so we can get the evanescent wave showed in figures.

According to the coupled mode equation [22], the coupled mode theory is introduced to explain this phenomenon. The differential form of coupled mode equation can be expressed as:

$$\begin{cases} \frac{dA_1(z)}{dz} = i\beta_1 A_1(z) + i\kappa_{21} A_2(z) \\ \frac{dA_2(z)}{dz} = i\beta_2 A_2(z) + i\kappa_{12} A_1(z) \end{cases} \quad (2)$$

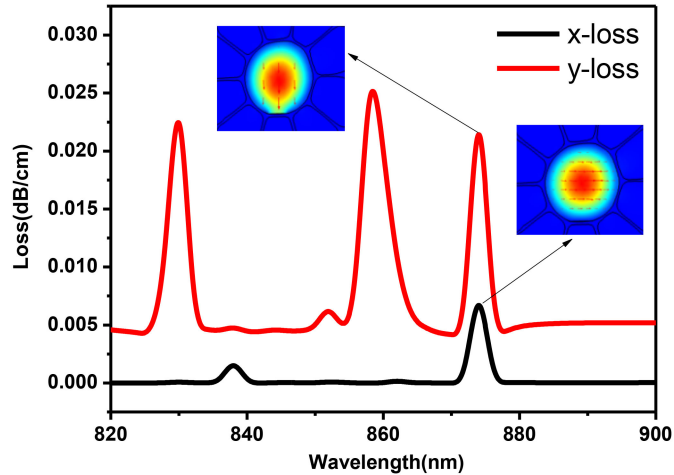


Fig. 2. The confinement loss in x and y directions respectively.

Where,  $\kappa_{12}$  and  $\kappa_{21}$  are the coupling coefficients between two waveguides, which is generally a complex number ignoring its own loss.  $A_1$  and  $A_2$  represent the mode fields of different modes and  $\beta_1$  and  $\beta_2$  are the corresponding modes. In optical waveguides,  $\kappa$  represents the coupling strength and  $\beta$  represents the propagation constant of coupled modes after coupling the two modes. By introducing them into equation (2), we can get:

$$\beta_{\pm} = \beta_{ave} \pm \sqrt{\delta^2 + \kappa^2}$$

While  $\beta_{ave} = (\beta_1 + \beta_2)/2$  and  $\delta = (\beta_1 - \beta_2)/2$ . For bound modes,  $\beta_1$  and  $\beta_2$  are both real. So  $\delta$  is also real. For leaky modes,  $\beta_1$  and  $\beta_2$  are both complexes. So  $\delta$  may also be complexes and written as  $\delta = \delta_r + i\delta_i$ . At phase matching point, the real parts of the two leaky mode propagation constants are equal, and in another word  $\delta_r = 0$ . It can be derived that:

$$\delta^2 + \kappa^2 = -\delta_r^2 + \kappa^2$$

When  $\delta_i < \kappa$ ,  $\beta_+$  and  $\beta_-$  have different real parts but equal imaginary parts and a complete coupling (regular anti-crossing) between two leaky modes happens. When  $\delta_i > \kappa$ ,  $\beta_+$  and  $\beta_-$  have equal real parts but different imaginary parts, and then an incomplete coupling appears. Combined with the energy distribution of the electric field, it can be seen that the y-polarized mode resonates at 835 nm, 860 nm, 875 nm, which transfers the energy confined to the core to the metal surface to a certain extent.

### 3. Experimental Results and Analysis

According to the experimental device below (Fig. 3), the polarization performance of the optical fiber was detected. Among them, the light source is an Ultra Wideband Light Source (NKT Photonics SL-300). Light is coupled to an ARF through a single-mode fiber (SMF) and a circular polarizer. Then polarized light is measured by an optical spectrum analyzer (OSA) through a single-mode fiber.

The loss of copper-free filled optical fibers is measured (as shown in Fig. 4a). The Broadband loss remains at a very low level of about 0.075 dB/cm, which confirms that there is no polarization effect in optical fibers. After copper coating, there are three absorption peaks at wavelength 835 nm, 860 nm and 875 nm (Fig. 4b) because of the SPR effect. The core loss increases, which is consistent with the theoretical results. The experimental value is higher than the theoretical value because of the additional loss caused by other factors in the experimental system.

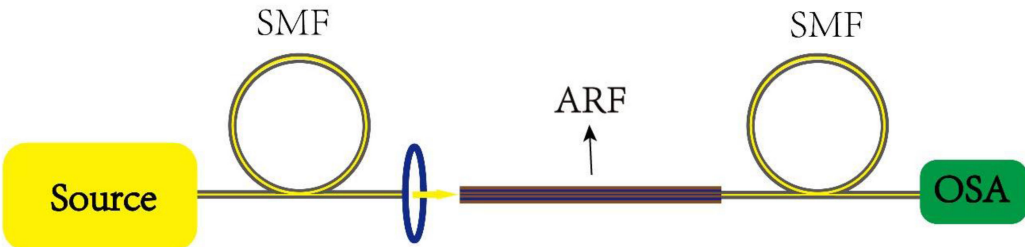


Fig. 3. The experimental setup for measuring polarization characteristics.

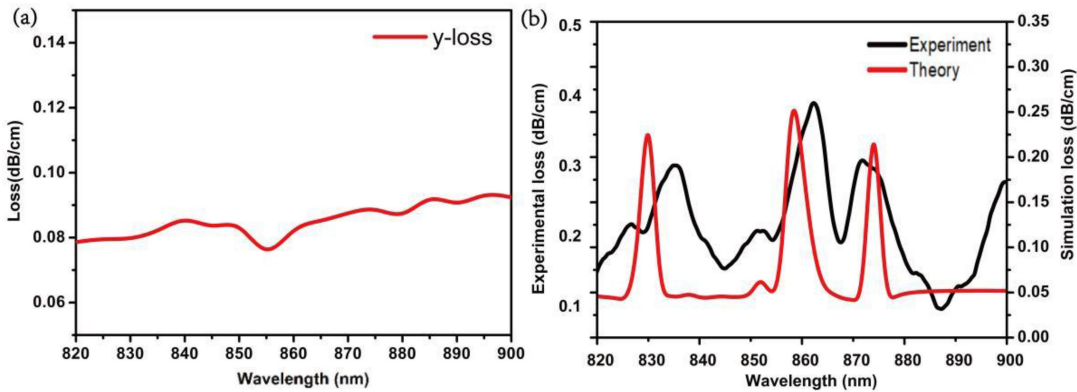


Fig. 4. Polarization loss. (a) Loss of fiber without copper. (b) Loss of fibers in experiment and theory coated with Cu film.

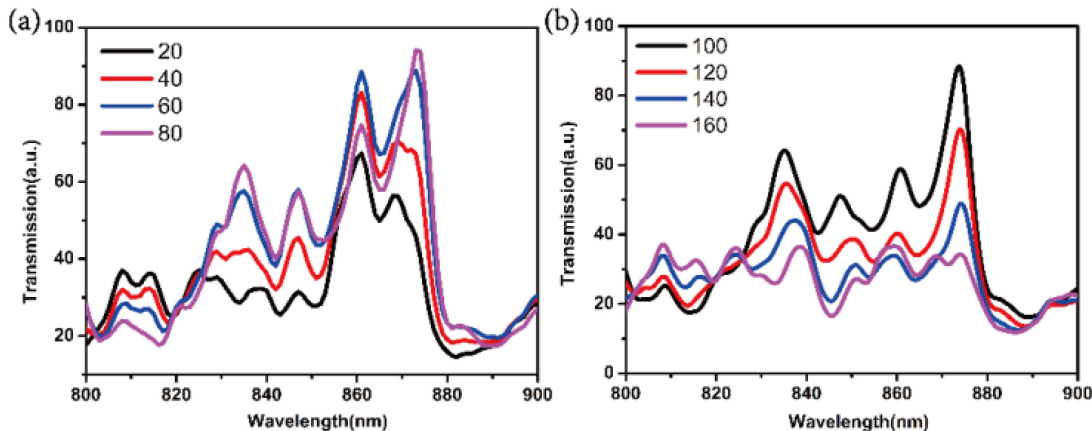


Fig. 5. Experimental polar diagram (a) Polarized light varying from 20° to 80°. (b) Polarized light varying from 100° to 160°.

In order to study the polarization characteristics of HC-ARF, the output spectra of optical fibers with a polarizer (GCM-0902M) rotating from 0° to 180° were measured (Fig. 5). In the reverse measurement, the polarizer rotates from 180° to 360°, and the results are similar to the forward rotation. The peak value of the output light is between 800 nm-900 nm, and the transmission spectrum of the output light varies linearly. It indicates that the output of the polarizer is indeed

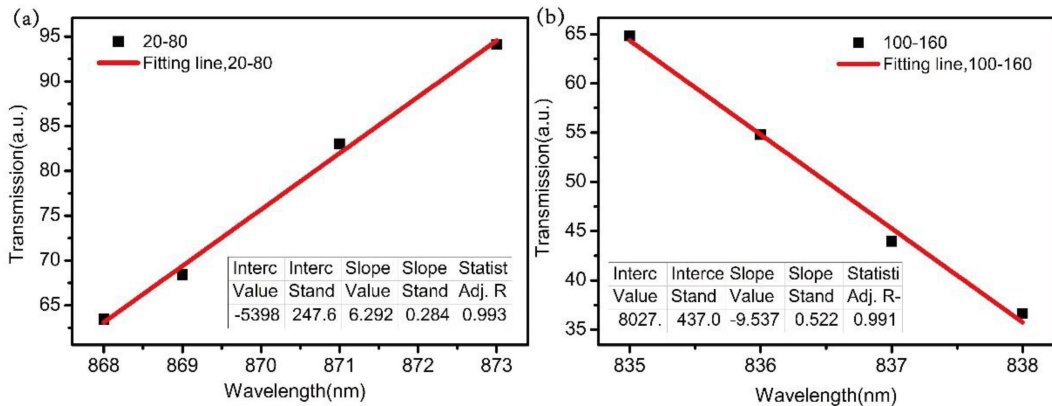


Fig. 6. Fitting line: (a) Linear fitting of transmission versus wavelength rotating from 20° to 80°. (b) Linear fitting of transmission versus wavelength rotating from 100° to 160°.

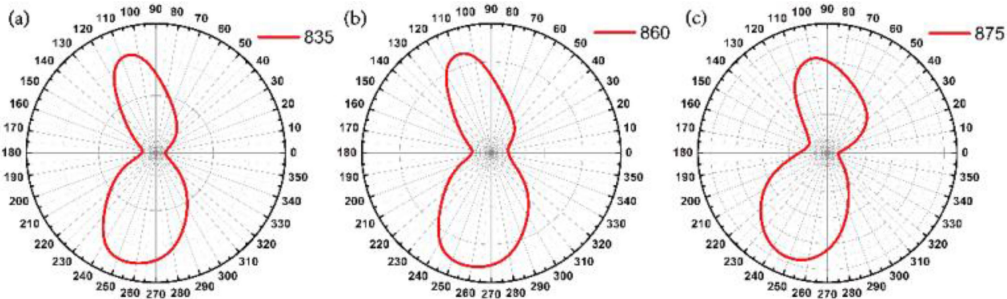


Fig. 7. The polarization property. (a) Polarized light at 835 nm with direction varying from 0° to 360°. (b) Polarized light at 860 nm with direction varying from 0° to 360°. (c) Polarized light at 875 nm with direction varying from 0° to 360°.

linearly polarized (Fig. 6). Regardless of the input polarization state, the output light of the polarizer maintains approximately linear polarization.

Fig. 7 shows the polarity diagram of the polarizer at different input polarizations, and the effect of the input polarization direction on the output ellipticity clearly. Fig. 7 a, b and c show the gradual change of the ellipticity of the output light under different input polarization wavelengths at 835 nm, 860 nm and 875 nm, respectively. As expected, the output of the polarizer has two maximum and minimum values, which can be used to produce high-performance polarized light. Therefore, the optical ellipticity in optical fibers has changed.

Crosstalk is an important parameter of the polarizer. It mainly determines the influence of the polarization direction which needs to be lost. The larger the crosstalk, the higher the transmission quality. To a certain extent, it can be used for the quality of polarization filtering. The greater the crosstalk, the higher the transmission quality. According to Bill's law [23] and the concept of crosstalk [24], the relationship between crosstalk (CT) and fiber length can be written as follows:

$$CT = 20 \lg \{ \exp [(\alpha_2 - \alpha_1)] L \} \quad (3)$$

Where  $\alpha_1$  and  $\alpha_2$  represent constrained losses in the X and Y directions respectively, and L shows the length of the optical fibers. When the optical fiber length is 1 mm, 1.5 mm and 2 mm, the peak strength and bandwidth of the intersection are shown in Fig. 8, and the intersection of devices increases with the increasing of the optical fiber length. Therefore, a polarizer with

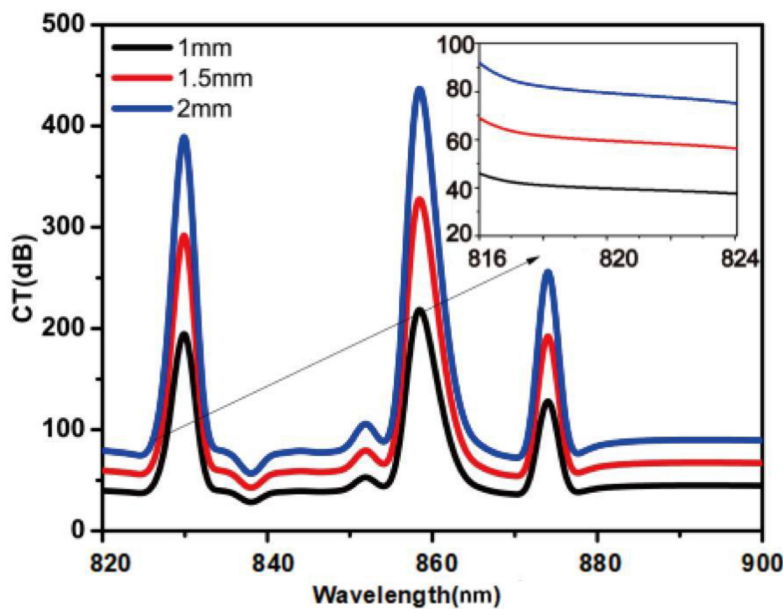


Fig. 8. The CT bandwidth of polarizer varies with the length of the fiber.

good performance can be realized by optimizing equipment length, manufacturing parameters, and manufacturing process. Compared to our previous work [25], the new hollow anti-resonant fiber has a more regular drawn structure which is easy to fabricate.

#### 4. Conclusions

In this paper, a kind of hollow-core anti-resonant fiber coated with copper on-line was fabricated by the fiber optic drawing tower. The polarization characteristics of hollow-core optical fibers are studied experimentally. By adjusting the parameters, the strong surface plasmon resonance (SPR) can be excited easily in the optical fiber. The polarization band of the optical fiber is between 820 nm and 900 nm. The experimental results are in agreement with the theoretical results. The experimental results show that the coupling between the core mode and SPP mode is very strong at 835, 860 and 875 nm. In addition, when the length of PCF changes, the crosstalk width will also increase. The polarity of the proposed structure under different input polarization was also measured. It shows that the fiber can produce linearly polarized light of different wavelengths. These excellent performances prove that the on-line coating method is of great value in the related field and they have good application value in communication, laser processing, and other fields.

---

#### Reference

- [1] M. Y. Azab, M. F. O. Hameed, A. M. Nasr, and S. S. A. Obayya, "Multifunctional plasmonic photonic crystal fiber biosensors," *Computational Photonic Sensors*. Cham, Switzerland: Springer, 2019, pp. 233–260.
- [2] F. Wiegandt *et al.*, "Quasi-phase-matched high-harmonic generation in gas-filled hollow-core photonic crystal fiber," *Optica*, vol. 6, no. 4, pp. 442–447, 2019.
- [3] J. C. Knight, "Photonic crystal fibres," *Nature*, vol. 424, no. 6950, pp. 847–851, 2003.
- [4] P. St. J. Russell, "Photonic-crystal fibers," *J. Lightw. Technol.*, vol. 24, no. 12, pp. 4729–4749, Dec. 2006.
- [5] S. G. Nelson, K. S. Johnston, and S. S. Yee, High sensitivity surface plasmon resonance sensor based on phase detection," *Sensors Actuators B, Chem.*, vol. 35, no. 1/3, pp. 187–191, 1996.
- [6] X. Zhao *et al.*, "Improvement of the sensitivity of the surface plasmon resonance sensors based on multi-layer modulation techniques," *Opt. Commun.*, vol. 335, pp. 32–36, 2015.
- [7] E. Klantsataya, P. Jia, H. Ebendorff-Heidepriem, T. M. Monro, and A. François, "Plasmonic fiber optic refractometric sensors: From conventional architectures to recent design trends," *Sensors*, vol. 17, no. 1, 2017, Art. no. 12.

- [8] H. W. Lee, M. A. Schmidt, and P. St. J. Russell, "Excitation of a nanowire ‘molecule’ in gold-filled photonic crystal fiber," *Opt. Lett.*, vol. 37, pp. 2946–2948, 2012.
- [9] J. Xue, S. Li, Y. Xiao, W. Qin, X. Xin, and X. Zhu, "Polarization filter characters of the gold-coated and the liquid filled photonic crystal fiber based on surface plasmon resonance," *Opt. Exp.*, vol. 21, no. 11, pp. 13733–13740, 2013.
- [10] J. Zi, S. Li, W. Zhang, and G. An, "Polarization filter characteristics of square lattice photonic crystal fiber with a large diameter gold-coated air hole," *Plasmonics*, vol. 10, no. 6, pp. 1499–1504, 2015.
- [11] R. K. Basak and D. Ghosh, "Polarization properties of selectively gold-filled suspended core microstructured optical fibers," *Plasmonics*, vol. 14, no. 6, pp. 1505–1517, 2019.
- [12] H. Li, S. Li, H. Chen, J. Li, G. An, and J. Zi, "A polarization filter based on photonic crystal fiber with asymmetry around gold-coated holes," *Plasmonics*, vol. 11, no. 1, pp. 103–108, 2016.
- [13] J. M. Fini *et al.*, "Polarization maintaining single-mode low-loss hollow-core fibres," *Nature Commun.*, vol. 5, 2014, Art. no. 5085.
- [14] S. A. Mousavi *et al.*, "Broadband high birefringence and polarizing hollow core antiresonant fibers," *Opt. Exp.*, vol. 24, no. 20, pp. 22943–22958, 2016.
- [15] C. Wei, C. R. Menyuk, and J. Hu, "Polarization-filtering and polarization-maintaining low-loss negative curvature fibers," *Opt. Exp.*, vol. 26, no. 8, pp. 9528–9540, 2018.
- [16] S. Yan, S. Lou, W. Zhang, and Z. Lian, "Single-polarization single-mode double-ring hollow-core anti-resonant fiber," *Opt. Exp.*, vol. 26, no. 24, pp. 31160–31171, 2018.
- [17] T. R. Woliński *et al.*, "Polarization properties of liquid crystal-core optical fiber waveguides," *Mol. Cryst. Liquid Cryst. Sci. Technol. A, Mol. Cryst. Liquid Cryst.*, vol. 352, no. 1, pp. 361–370, 2000.
- [18] W. Qian *et al.*, "A proposal of a novel polarizer based on a partial liquid-filled hollow-core photonic bandgap fiber," *Opt. Commun.*, vol. 284, no. 19, pp. 4800–4804, 2011.
- [19] M. F. O. Hameed *et al.*, "Ultra-high tunable liquid crystal-plasmonic photonic crystal fiber polarization filter," *Optics Exp.*, vol. 23, no. 6, pp. 7007–7020, 2015.
- [20] G. P. Agrawal, *Nonlinear Fiber Optics*. New York, NY, USA: Academic, 2007.
- [21] V. G. Kravets, P. Y. Kurioz, and L. V. Poperenko, "Spectral dependence of the magnetic modulation of surface plasmon polaritons in permalloy/noble metal films," *J. Opt. Soc. Amer. B*, vol. 31, pp. 1836–1844, 2014.
- [22] Z. Zhang *et al.*, "Dependence of leaky mode coupling on loss in photonic crystal fiber with hybrid cladding," *Opt. Exp.*, vol. 16, pp. 1915–1922, 2008.
- [23] J. C. Zi *et al.*, "Polarization filter characteristics of square lattice photonic crystal fiber with a large diameter gold-coated air hole," *Plasmonics*, vol. 10, pp. 1499–1504 (2015).
- [24] H. Li *et al.*, "A polarization filter based on photonic crystal fiber with asymmetry around gold-coated holes," *Plasmonics*, vol. 11, pp. 103–108, 2016.
- [25] B. Li *et al.*, "Surface plasmon resonance on the V-Type microstructured optical fiber embedded with dual copper wires," *Plasmonics*, vol. 14, no. 2, pp. 383–387, 2018.